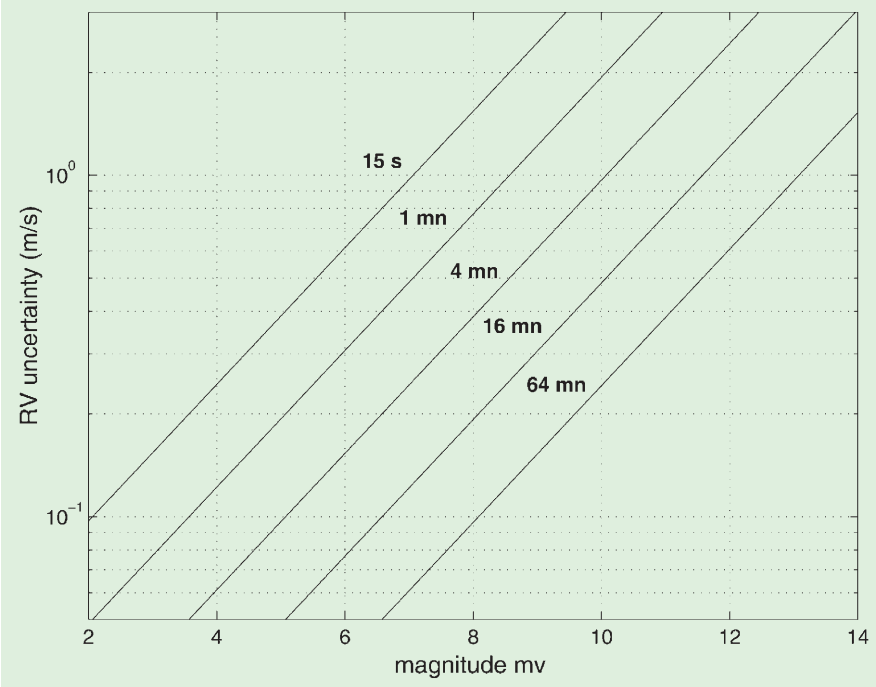

Figure 11: Radial velocity uncertainty predictions for HARPS versus magnitude for a star spectrum with T_{eff} = 4500 K and v sin i = 0 km s^{-1}.

is presented in Figure 10 versus effective temperature and rotational broadening. Figure 11 shows the photon noise uncertainty versus stellar magnitude for the best stellar case (T_{eff} = 4500 K, *v* sin *i* = 0 km s^{-1}) for various exposure times. This quantity is less than 1 m s^{-1} for exposure time of 1 mn on stars with magnitude lower than 8. Typically, a gain of 5 magnitudes is expected compared to CORALIE.

UVES (Ultraviolet and Visual Echelle Spectrograph) is a cross-dispersed echelle spectrograph located at the second Unit Telescope of the 8.2-m ESO VLT. FLAMES (Fibre Large Array Multi Element Spectrograph) is a VLT large-field fibre facility that consists of several components, including a fibre link to the UVES spectrograph. The light is collected at the Nasmyth focus through 8 fibres in a usable field of up to 25 arcmin in diameter. Considering that one fibre is used for the simultaneous Thorium spectrum, 7 objects can be simultaneously measured with UVES. The photon-noise study for HARPS has been extrapolated to UVES and shows a gain between 1 and 2 magnitudes.

All these prospects show that Doppler ground-based asteroseismology will undergo intensive developments these next years and will be able to enlarge our understanding on stellar physics.

Acknowledgements

We would like to thank M. Mayor who encourages our programme and gives us time allocation at the Euler Swiss telescope. D. Queloz and all people associated with the CORALIE and HARPS projects are acknowledged for their help and for ongoing discussions and helpful comments.

References

Baranne, A., Queloz, D., Mayor, M., et al., 1996, *A&ASS*, **119**, 373.

Bouchy, F., & Carrier, F., 2001, *A&A*, **374**, L5.

Bouchy, F., Pepe, F., Queloz, D., 2001, *A&A*, **374**, 733.

Bedding, T.R., Butler, R.P., Kjeldsen, H., et al., 2001, *ApJ*, **549**, L105.

Carrier, F., Bouchy, F., Kienzle, F., & Blecha, A., 2001a, IAU 185, ASP Conf. Ser., in press.

Carrier, F., Bouchy, F., Kieuzle, F., et al., 2001b, *A&A*, **378**, 142.

Carrier, F., Bouchy, F., Provost, J., et al., 2001c, IAU 185, ASP Conf. Ser., in press.

Grec, G., Fossat, E., Pomerantz, M.A., 1983, *Solar Physics*, **82**, 55.

Guenther, D.B., & Demarque, P., 2000, *ApJ*, **531**, 503.

Kjeldsen, H., & Bedding, T., 1995, *A&A*, **293**, 87.

Leighton, R.B., Noyes, R.W., & Simon, G.W., 1962, *ApJ*, **135**, 474.

Martic, M., Schmitt, J., Lebrun, J.-C., et al., 1999, *A&A*, **351**, 993.

Morel, P., Provost, J., Lebreton, Y., et al., 2000, *A&A*, **363**, 675.

Pallé, P., 1997, Proc. IAU Symp. 181, Provost & Schmider (eds), 15.

Queloz, D., Mayor, M., Weber, L., et al., 2000, *A&A*, **354**, 99.

Queloz, D., Mayor, M., et al., 2001, *The Messenger*, **105**, 1.

Setiawan, J., Pasquini, L., da Silva, L., et al., 2000, *The Messenger*, **102**, 13.

Ulrich, R.K., 1970, *ApJ*, **162**, 993.

Discovery of Lead Stars with the ESO 3.6-m Telescope and CES

S. VAN ECK (Institut d'Astronomie et d'Astrophysique, Université Libre de Bruxelles), svaneck@astro.ulb.ac.be

S. GORIELY and A. JORISSEN (Institut d'Astronomie, Bruxelles), and B. PLEZ (GRAAL, Montpellier)

1. The Synthesis of Elements Heavier than Iron in Stars

In a seminal paper, Burbidge et al. (1957) lay the foundations of our understanding of the origin of the elements heavier than iron: these elements cannot be formed by the mainstream nucleosynthesis processes feeding the stellar energy. They require instead that pre-existing seed nuclei, like the abundant iron-group elements, form heavier and heavier nuclei by successive captures of neutrons. In this neutron-capture chain, unstable nuclei are formed. Depending on the respective time scales for β-decay and neutron-capture (respectively τ_β and τ_n), the neutron-capture process will either be dubbed slow (s-process: $\tau_\beta < \tau_n$) or rapid (r-process: $\tau_\beta > \tau_n$). The r-process occurs during the supernova event, and is able to produce heavy elements up to the actinides (Th, U). These actinides are injected into the interstellar medium by the supernova remnant, and are subsequently incorporated into the next

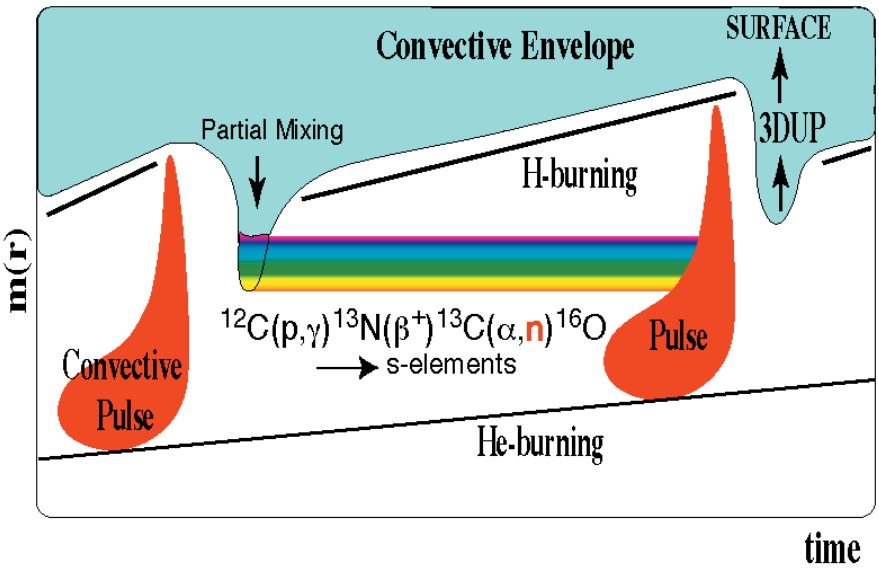

Figure 1: Temporal evolution of the structure of the intershell region of an AGB star, sketching the partial proton mixing in the He intershell zone, and the subsequent s-process nucleosynthesis occurring in the region depicted with rainbow colours.

generation of stars, at the surface of which they may be observed. A success in that story has recently been achieved by a member of this team (BP) who reported the detection of Uranium in the atmosphere of a very metal-poor star using UVES (Cayrel et al. 2001).

The s-process operates in stars either during core He-burning in massive stars (Prantzos et al. 1987) or during the asymptotic giant branch (AGB) phase in the evolution of low- and intermediate-mass stars (e.g., Gallino et al. 1998). At that phase, stars develop a complex structure, consisting of a degenerate core, H- and He-burning layers, and a deep convective envelope (Fig. 1). The double-shell structure is thermally unstable, with a thermal runaway ('thermal pulse') occurring recurrently in the He-burning layer. The energy liberated by this thermal pulse disturbs the envelope, which then relaxes through a temporary deepening of its lower boundary. The convective envelope then penetrates the intershell region where He-burning operated in a convective pocket associated with the thermal pulse (Fig. 1). With this mixing process, called the 'third dredge-up' (3DUP), elements produced in the intershell zone are brought into the convective envelope, and hence become visible at the stellar surface. Carbon stars are formed in this way during the AGB.

Neutrons may possibly be produced in this context through the reaction chain $^{12}C(p,\gamma)^{13}N(\beta)^{13}C(\alpha,n)^{16}O$ if protons from the hydrogen shell can be partially mixed downward into the intershell zone enriched in ^{12}C from the former thermal pulse.

Recent studies (Herwig et al. 1997, Langer et al. 1999) have suggested that the transport processes accompanying the 3DUP could induce the required partial mixing of protons (PMP).

Although this scenario is nowadays the most widely accepted one, its main ingredient (the partial mixing of protons in the deep carbon-rich layers) cannot yet be derived from first physical principles due to the difficulties inherent to the description of convection, diffusion or rotational transport in 1-D models.

It is therefore of prime importance to devise predictions that may test this proton mixing scenario against abundance observations. Although the presence of the unstable element Tc (whose isotope ^{99}Tc is produced by the s-process and has a half life of only 2.1×10^5 y) at the surface of S stars (e.g., Van Eck & Jorissen 1999) clearly indicates that the s-process takes place in these AGB stars, it does not provide strong constraints on its detailed operation. A more stringent prediction, expressed by Goriely & Mowlavi (2000ab), is that low-metallicity AGB stars should exhibit large overabundances of Pb-Bi as compared to lighter s-elements. This is because at low metallicities the pre-existing seed nuclei are comparatively less abundant, so that the available neutrons are then numerous enough to convert all the seed nuclei into Pb and Bi. Within the PMP scenario, the prediction that [Pb/s] should be large (where $[A/X] \equiv \log(N_A/N_X) - \log(N_A/N_X)_\odot$, and s stands for any element produced by the s-process) is found to be quite robust with respect to the model parameters (like the abundance profile of the protons in the partially mixed layers, or the extent of the partial mixing zone) and uncertainties (e.g., reaction rates). All s-process enriched AGB stars with metallicities $[Fe/H] \leq -1.3$ are thus predicted to be 'Pb stars' (Goriely & Mowlavi 2000a), independently of their mass or metallicity (provided the partial mixing of protons takes place). 'Pb stars' are characterised not only by large [Pb/Fe] and [s/Fe] abundance ratios, but also by large [Pb/s] abundance ratios. In particular, [Pb/hs] (where hs denotes the so-called heavy s-process elements such as Ba, La or Ce) ratios as large as 1.5 are predicted by Goriely & Mowlavi (2000a) in AGB stars with $[Fe/H] \leq -1.3$.

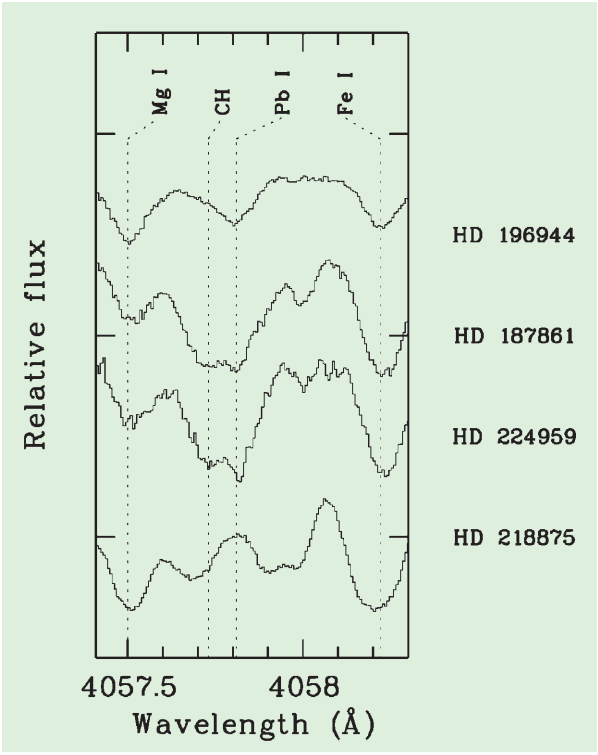

Figure 2: The CES spectra were obtained with the medium-resolution image slicer and the thinned, back-side illuminated CCD#61 (EEV, 2K × 4K pixels) yielding a resolution of 135,000; exposure times lie in the range 1 h 30 to 2 h 30. Note how strong the Pb I λ405.781 nm line is in the three CH stars. It is absent in the comparison R star HD 218875 (lower spectrum).

2. Observations: A Success Story

With this prediction about the existence of Pb stars in hand (first presented at the 1999 Liège Astrophysical Colloquium: Goriely & Mowlavi 2000b), we rushed to introduce an ESO observing

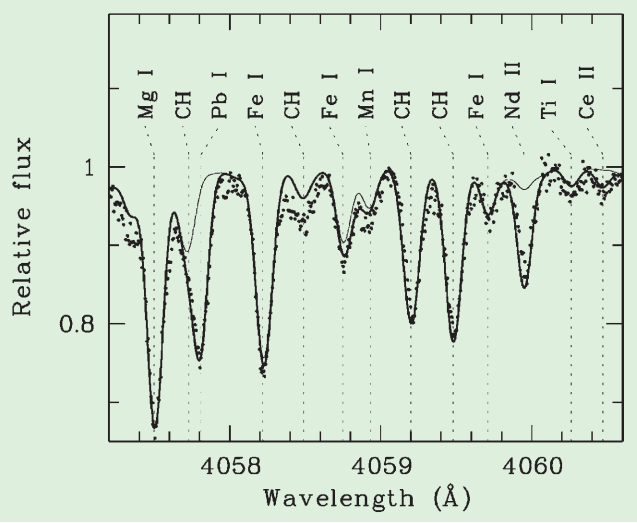

Figure 3: Comparison between the observed spectrum of HD 196944 with synthetic spectra corresponding to [s/Fe] = 0 (thin solid line; in this case the Pb line is not visible) and with the best matching [s/Fe] abundance set as given by Van Eck et al. (2001; thick solid line).

proposal. Luck was then with us twice: first when time was allocated at once to our project by the OPC, and second when the finishing Chilean winter offered us two good nights in September 2000. The Very Long Camera of the CES fed by the 3.6-m telescope provides the ideal instrumental set-up for testing our prediction. Although the recently refurbished CES/VLC (Kürster 1998ab) offers a resolution as high as R = 235,000, we chose R = 135,000 as a compromise between resolution and sensitivity. This set-up already allows us to separate the Pb I λ405.781 nm line from a CH line lying less than 0.1 Å bluewards.

As genuine low-metallicity AGB stars are rare in the solar neighbourhood, the target list comprised CH stars instead, a class of low-metallicity binary stars whose atmosphere bears the evidence for pollution by s-process-rich matter, probably coming from their companion formerly on the AGB (now a dim white dwarf; McClure & Woodsworth 1990).

At the telescope, it was immediately obvious that all the CH stars targeted by the programme had a very strong Pb I line. Figure 2 compares the CES/VLC spectra of CH stars with that of a warm carbon comparison star of spectral type R which does not appear to be enriched in lead.

The abundances were derived from spectral synthesis in the 404.5–407.1 nm spectral window using POSMARCS model atmospheres (Plez et al. 1992) matching their CNO abundances and metallicity. Solar oscillator strengths were derived from a synthesis of the solar spectrum, except for the 405.781 nm Pb I line, for which the laboratory value log gf = –0.22 has been adopted (Biémont et al., 2000). Although efforts were made to improve upon existing CN and CH line lists, the larger errors affecting the abundances in the two carbon-rich stars (HD 187861 and HD 224959, see Figure 4 and Van Eck et al. 2001) are mainly due to remaining inaccuracies in the CN line list.

3. Comparison with Predicted Abundances

Figure 4 presents the abundance pattern derived as described in Van Eck et al. (2001) for our three CH stars which have metallicities in the range –2.45 ≤ [Fe/H] ≤ –1.65, and compared to the predictions for the operation of the PMP in AGB stars of the same metallicities (see Goriely & Mowlavi 2000a for details about the models). Despite the fact that few elements have useful lines in the narrow (26 Å) spectral window offered by the CES/VLC around the Pb I line, the available data are in very good agreement with the PMP predictions.

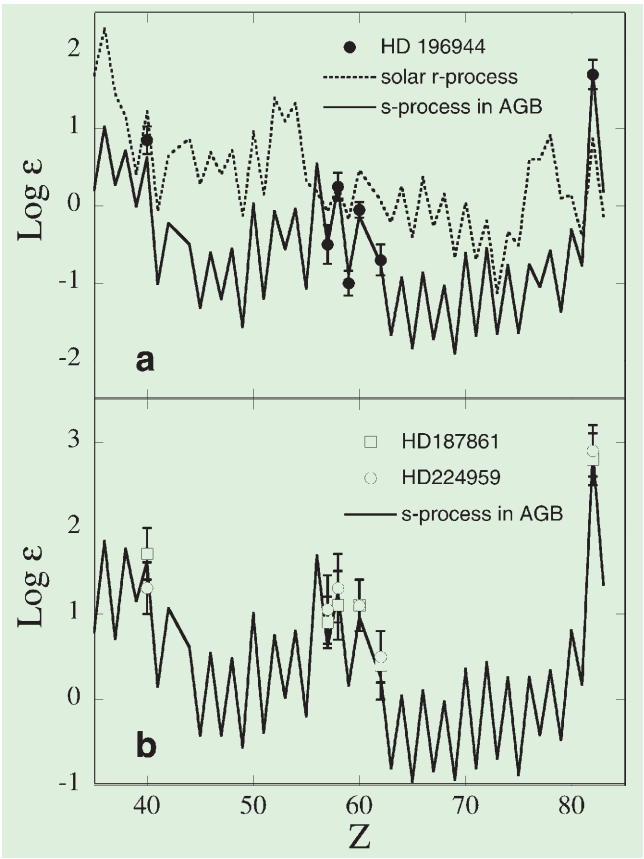

Figure 4: Comparison of the observed abundances with PMP abundance predictions. The model abundances are obtained as described in Goriely & Mowlavi (2000a) for stars of the same metallicities as the programme stars. The abundances are given in the scale log(ε_H) = 12. The upper panel (a) displays as well the solar system r-abundance distribution normalised to Ce. This comparison clearly shows that the large [Pb/hs] ~ 1.2 abundance ratio cannot be understood in terms of an r-process enrichment.

Although this good agreement strongly supports the PMP mechanism for the operation of the s-process in AGB stars, alarm signals came in at about the same time from the observations by Aoki et al. (2001) of [Pb/hs] ratios not larger than 0.4 (despite large Pb overabundances of the order of [Pb/Fe] = 2.3 to 2.6) in the slightly more metal-deficient carbon stars LP 625-44 and LP 706-7 ([Fe/H] about –2.7). Since these [Pb/hs] ratios are incompatible with the seemingly robust predictions from the PMP mechanism, they raise the questions whether the s-process operates in totally different ways in AGB stars with metallicities above and below [Fe/H] of about –2.5, as suggested by Fujimoto et al. (2000).

4. Future Prospects

The faintness of many other good candidate lead stars strongly limited the target list for the 3.6-m telescope and CES. UVES offers better prospects both on the ground of limiting magnitude and of spectral coverage. Its good UV sensitivity opens the way to the study of other Pb I lines lying in the UV, as well as of many other heavy elements.

The different abundance patterns observed among very low-metallicity, s-process-rich stars will undoubtedly stimulate the nucleosynthesis modelling of AGB stars of low (or even zero) metallicity, as initiated by Fujimoto et al. (2000) and followed by many other works since then (e.g., Goriely & Siess, 2001).

Finally, our data will help to fix the Pb yields from low-mass stars at low metallicities, that may then be used in models of the chemical evolution of the Galaxy (e.g., Travaglio et al. 1999). This would make the splitting between the s- and r-contribution to the solar Pb possible.

Acknowledgement

It is a pleasure to thank Dr. M. Kürster and the whole 3.6-m team for their operational support.

References

Aoki, W., Ryan, S.G., Norris, J.E., et al., 2001, *ApJ*, in press (astro-ph/0107040).

Biémont, E., Garnir, H. P., Palmeri, P., Li, Z. S. & Svanberg, S., 2000, *Mon. Not. R. Astron. Soc*. **312**, 116–122.

Burbidge, E.M., Burbidge, G.R., Fowler, W.A., Hoyle, F., 1957, *Rev. Mod. Phys.* **29**, 547.

Cayrel, R., Hill, V., Beers, T. C., et al., 2001, *Nature* **409**, 691.

Fujimoto, M.Y., Ikeda, Y., Iben, I.Jr. 2000, *ApJ* **529**, L25.

Gallino, R., Arlandini, C., Busso, M., et al., 1998, *ApJ* **497**, 388.

Goriely, S., Mowlavi, N., 2000a, *A&A* **362**, 599.

Goriely, S., Mowlavi, N., 2000b, in "The Galactic Halo: From Globular Clusters to Field Stars", A. Noels P. Magain, D. Caro, E. Jehin, G. Parmentier, A. Thoul (eds.), Proc. of the 35th Liège Intern. Astrophys. Coll. (Université de Liège, Belgium), 25.

Goriely, S., Siess, L., 2001, *A&A* **378,** L25.

Herwig, F., Blöcker, T., Schönberner, D., El Eid, M., 1997, *A&A* **324**, L81.

Kürster, M., 1998a, *The Messenger* **92**, 18.

Kürster, M., 1998b, *The Messenger* **94**, 12.

Langer, N., Heger, A., Wellstein, S., Herwig, F., 1999, *A&A* **346**, L37.

McClure, R.D., Woodsworth, A.W., 1990, *ApJ* **352**, 709.

Plez, B., Brett, J.M., Nordlund, A., 1992, *A&A* **256**, 551

Prantzos, N., Arnould, M., Arcoragi, J.-P., 1987, *ApJ* **315**, 209.

Travaglio, C., Galli, D., Gallino, R., et al., 1999, *ApJ* **521**, 691.

Van Eck, S., Jorissen, A., 1999, *A&A* **345**, 127.

Van Eck, S., Goriely, S., Jorissen, A., Plez, B., 2001, *Nature* **412**, 793.

SIMBA Explores the Southern Sky

L.-Å. NYMAN and M. LERNER, SEST and Onsala Space Observatory
M. NIELBOCK, M. ANCIAUX and K. BROOKS, ESO
R. CHINI, M. ALBRECHT and R. LEMKE, Astronomical Institute of Ruhr University of Bochum
E. KREYSA and R. ZYLKA, Max Planck Institute for Radio Astronomy
L.E.B. JOHANSSON, Onsala Space Observatory
L. BRONFMAN, Department of Astronomy, University of Chile
S. KONTINEN, Observatory, University of Helsinki
H. LINZ and B. STECKLUM, Thüringer Landessternwarte Tautenburg

SIMBA

SIMBA (the SEST Imaging Bolometer Array) was installed on the SEST in June this year through a collaboration between the University of Bochum, the Max-Planck-Institute for Radio Astronomy, the Swedish National Facility for Radio Astronomy and ESO. It is a 37-channel bolometer array operating at a wavelength of 1.2 mm.

Images produced by SIMBA are taken with the telescope in a fast scanning mode with speeds up to 160″/s without using a nutating subreflector. The beam size of SEST is 24″ at 1.2 mm and the pixel size in the SIMBA maps presented here is set to 8″. A map with a size of 15′ by 6′ with a rms noise of 40–50 mJy is obtained in only 12 minutes. More technical information about SIMBA is given on the SEST home page, and preliminary results were presented in ESO Press Release 20/01.

The strength of SIMBA is certainly the efficient coverage of large areas in a short time. It has therefore been used to map and survey regions of star formation in our own Galaxy as well as in nearby galaxies where cold dust and ionised regions emit strongly at 1.2 mm wavelength. SIMBA has also been used to study planetary nebulae, quasars, and maps of the deep fields in the Southern sky (the Hubble deep field South, the Chandra deep field, and the Phoenix deep field) have been obtained.

The SIMBA images presented in this article are preliminary in the sense that they were reduced with the on-line data reduction system. The data reduction software MOPSI – which so far has only been used for data obtained with a chopping secondary – is presently being adapted to the fast scanning mode and it is expected that all existing maps will improve in terms of intensity calibration and noise performance. Consequently, parts of extended, faint emission might have escaped detection so far but should appear more frequently after the upgrade.

The Orion region

Figure 1 displays the SIMBA map of the entire integral shaped Orion A molecular cloud complex at a wavelength of 1.2 mm. It has been created from 13 single maps during a total integration time of about 3.5 hours. The 1-sigma residual noise is about 40 mJy/beam.

The Orion A complex is usually divided into three regions, known as OMC-1, OMC-2 and OMC-3 (right panel), and the Orion Nebula (M 42) which belongs to the most luminous HII regions known. M42 is located in front of OMC-1 at a distance of 470 pc. This region also encompasses the brightest millimetre peaks of the SIMBA map, coincident with the Becklin-Neugebauer (BN) object adjacent to the Kleinmann-Low (KL) Nebula. The BN object is thought to be a young massive star of about 25 $L_{\odot}$ with a considerable mass loss.

Both M 42 and OMC-1 are regions of current massive star formation. OMC-1 itself is heated by stars from the nearby OB cluster within the Orion Nebula, including the Orion Trapezium. Its UV radiation is also responsible for photodissociation regions (PDR) on the surface of OMC-1 and southern parts of OMC-2.

OMC-2 and OMC-3 also show star-formation activity which is obvious from the numerous dense cores located within the filament. Some of them coincide with VLA radio sources, which is usually a sign of free-free emission from bow shocks of protostellar molecular outflows. In contrast to OMC-1, however, preferably low-mass stars are created there. Both OMC-2 and OMC-3 possess comparable amounts of gas and dust, although OMC-3 seems to be less evolved than OMC-2. Six of ten compact millimetre sources in OMC-3 have been identified as Class 0 protostars, while all sources in OMC-2 are at least of Class I. Furthermore, temperatures are lower and outflows are less